Microsystem Technologies (2021) 27:2873–2887
https://doi.org/10.1007/s00542-020-05091-2

TECHNICAL PAPER

A multilayered photonic emitter for high-performance daytime radiative cooling

Adil Mohammed[1] · Sumith Yesudasan[2] · Sibi Chacko[1]

Received: 3 September 2020 / Accepted: 1 November 2020 / Published online: 16 November 2020

Abstract
Daytime radiative cooling devices consisting of various materials are used to transmit and radiate heat energy from a target body outward through the atmosphere and into cold outer space, without using external energy and in the presence of sunlight. In this study, a daytime radiative cooling thin film structure is designed to achieve high emission in the atmospheric transparency window (8–13 μm) and a high reflection of solar radiation. Simple and chemically stable inorganic materials of silicon dioxide, silicon nitride, aluminum oxide, and silver are selected for the initial design of the structure, initially having four layers. The needle optimization technique is used to enhance the initial design to acquire a final structural design of 10 layers of the selected materials. The average emissivity of the cooler in the range of 8–13 μm was numerically found to be 94.5% and the average reflectance for the solar spectrum was determined to be 96.3% according to validated calculations. Lastly, a high net cooling performance of 125 W/m^2 is theoretically generated by the structure when it is equal to the ambient temperature and a temperature reduction of 8 °C is achieved from the ambient temperature according to validated calculations.

1 Introduction

Cooling systems are an essential requirement in our daily lives as they can be used to remove and dissipate heat energy from almost any kind of undesirable heat source. However, the use of such systems generally requires a significant amount of external energy and results in high greenhouse gas emissions which leads to global warming, which consequently has a harmful impact on the environment of the planet. This has led to the introduction of various novel ideas in the field of passive cooling, or cooling without any external or active source of energy (Daisy 2016). Recent studies have focused on the phenomenon of radiative cooling, a passive cooling approach that lowers the temperature of surfaces exposed to sunlight, without causing emissions and without using external energy (Ko et al. 2018).

Radiative cooling or sky cooling is a phenomenon by which cooling of a surface or a body occurs through the process of radiation. It occurs naturally during the night when sunlight or solar energy is not present. In general, radiation is the emission of energy in the form of electromagnetic waves, caused by the presence of heat energy in a body. Most of the heat energy emitted by a body is in the form of infrared radiation. The heat energy emitted in the form of infrared radiation of certain wavelengths can pass through the atmosphere and reach cold outer space. This is because the atmosphere does not absorb this energy and is instead transferred from the atmosphere in the form of radiation into outer space (Ko et al. 2018; Santamouris and Feng 2018).

The main challenge is to radiate this form of heat energy in the presence of sunlight, which normally counteracts the effect of radiative cooling. Specific materials in the form of a film or a coating can be used to radiate heat energy into the atmosphere in the presence of sunlight, due to certain optical properties that manipulate the movement of light and generate a cooling effect. As a result, radiative cooling is an exceptional idea as it can generate a cooling effect

✉ Sumith Yesudasan
sumith.yesudasan@shsu.edu

Adil Mohammed
am302@hw.ac.uk

Sibi Chacko
c.sibi@hw.ac.uk

[1] School of Engineering and Physical Sciences, Heriot-Watt University, Academic City, Dubai, UAE

[2] Department of Engineering Technology, Sam Houston State University, Huntsville, TX, USA

without external energy; is beneficial to the environment as an alternative approach to cooling and can occur in the presence of sunlight during daytime. Radiative cooling can also be used to absorb unwanted heat from other sources and emit this heat in the form of radiation into space.

A radiative cooler that does not need an active energy source and which can produce a high cooling performance during daytime can be used for various applications. Recently, passive daytime radiative coolers have been considered for the dissipation of heat from semiconductor devices such as solar cells, or as a cooling strategy for buildings to help reduce power consumption(Santamouris and Feng 2018; Babu et al. 2020). The efficiency of solar cells decreases when it reaches high temperatures of around 50–55 °C, this can occur if the solar cell is exposed to strong sunlight (Jeong 2020a). Additionally, the lifetime of the solar cell can be shortened due to strong sunlight. To prevent these problems, a daytime radiative cooler can be integrated within the solar cell which would help it cool passively and not let its temperature increase beyond operating limits. Moreover, passive cooling has been shown to reduce the dry-bulb temperature of water by 3–5 °C (Jeong et al. 2020a).

A cooling system using passively chilled water was shown to increase the energy savings of a building by 21% after conducting a building energy simulation (BES) (Jeong et al. 2020a; Goldstein et al. 2017; Noronha et al. 2020). The water is cooled using passive daytime radiative cooling, which saves the energy of the building by requiring lesser cooling energy from an active source. More research was performed in a study on the application of photonic radiative cooling in indoor cooling systems of buildings. According to the study, 68% of the energy required for cooling within buildings in the USA can be saved using a photonic radiative cooler (Jeong et al. 2020a; Wang et al. 2018). In another study, the idea of a daytime radiative cooler integrated with an HVAC (heating, ventilation, air-conditioning) system using only one refrigeration cycle was proposed. The novel system uses water after being cooled by radiative cooling to reduce the indoor temperature of air and is expected to have a net cooling power of 1600 W and decrease the air temperature by 10 °C (Jeong et al. 2018, 2020a). Researches are also focused on the nanoscale domain to investigate the possibility of passive cooling devices (Yesudasan and Chacko 2018; Yesudasan et al. 2020; Sumith and Maroo 2015, 2016; Hotchandani et al. 2020).

In this work, a photonic emitter based cooling device concept is proposed with the support of numerical investigation. The proposed device can transfer thermal energy to space without any external power supply and connections. The conceptual device is promising for futuristic cooling devices and can be used at different length scales ranging from nanoscale (Yesudasan and Chacko 2018) to large scales (Sumith and Maroo 2016).

2 Literature review

2.1 Background theory

The process of heat rejection from a body through radiative cooling is based on certain principles. Firstly, the atmosphere has a property of selective emission for the entire spectrum of electromagnetic radiation (Hossain and Gu 2016). This means that the atmosphere selectively allows certain wavelengths of radiation to pass through it, and this varies throughout its range of altitude. A range of wavelength exists from 8 to 13 μm, in which the atmosphere is transparent, which means that radiation in this range can completely pass through it and can reach outer space (Raman et al. 2014). Therefore, this wavelength range is considered for thermal radiation from the body, and it is present within the infrared spectrum of electromagnetic radiation. As such, the heat energy emitted is mainly in the form of infrared radiation. Lastly, for any type of heat transfer, heat energy always flows from a high-temperature source to a low-temperature sink. In this case, the high-temperature source is the hot surface of the body and the low-temperature sink is the cold vast space of the universe that has a temperature of around 3 K (Chen et al. 2016). Radiative cooling according to these concepts results in passive or energy-free cooling of the surface.

During daytime, electromagnetic radiation ranging from visible to infrared is incident on the target surface. The high wavelength infrared range of 8–13 μm is considered for thermal emission. The remaining wavelengths which include the visible and near-infrared spectrums need to be reflected away. As a result, to achieve effective passive cooling, a surface coating should be designed such that it can emit in the 8–13 μm range and reflect in the visible and near-infrared spectrums of radiation.

For the calculation of radiative cooling power, a radiative cooler of surface area 'A' at a temperature 'T' with a spectral and angular emissivity given by $\epsilon(\lambda, \theta)$ needs to be considered. When the cooling film is subject to sunlight, it is affected by solar irradiance and atmospheric thermal radiation. The parameters for atmospheric radiation include the ambient temperature of the surroundings T_{amb} and the emissivity of the atmosphere $\epsilon_{atm}(\lambda, \theta)$.

The net radiative cooling power of a thin-film cooler is calculated using the following equation:

$$P_{cool}(T) = P_{rad}(T) - P_{atm}(T_{amb}) - P_{sun} - P_{cond+conv} \quad (1)$$

In the above equation, the radiative power of the cooling device (P_{rad}) is given by:

$$P_{rad}(T) = A \int d\Omega \cdot \cos\theta \int_0^{\infty} d\lambda \cdot I_{BB}(T,\lambda) \cdot \epsilon(\lambda,\theta) \tag{2}$$

where $\int d\Omega = 2\pi \int_0^{\pi/2} d\theta \sin\theta$ is the angular integral over a hemisphere, and

$$I_{BB}(T,\lambda) = \frac{2hc^2}{\lambda^5} \frac{1}{e^{hc/\lambda k_B T} - 1} \tag{3}$$

is the expression for the spectral radiance of a black body at a temperature T. Here, h is Planck's constant, k_B is the Boltzmann constant, λ is the wavelength, and c is the speed of light. For a range of wavelength, the radiated power is calculated by changing the limits of the wavelength integral in Eq. (2), as shown in the equation below:

$$P_{rad}(T) = A\pi \int_{\lambda 1}^{\lambda 2} \frac{2hc^2}{\lambda^5} \frac{1}{e^{hc/\lambda k_B T} - 1} d\lambda \cdot \epsilon(\lambda,\theta) \tag{4}$$

The atmospheric thermal radiative power absorbed by the atmosphere is given by:

$$P_{atm}(T_{amb}) = A \int d\Omega \cdot \cos\theta \int d\lambda \cdot I_{BB}(T_{amb},\lambda) \cdot \epsilon(\lambda,\theta) \cdot \epsilon_{atm}(\lambda,\theta) \tag{5}$$

$$\epsilon_{atm} = 1 - t^{1/\cos\theta} \tag{6}$$

The atmospheric emissivity is calculated from atmospheric transmittance in the zenith direction. The data of the spectral behavior of the transmission of the atmosphere is obtained from an external source (The Sites|Gemini Observatory 2020). It should be known that the atmospheric transmittance data from (The Sites|Gemini Observatory 2020) are for high elevation observatories with transparent atmospheric conditions. The atmospheric transmittance could likely be lower for conventional locations or typical atmospheric conditions (Berdahl et al. 1983; Martin and Berdahl 1984).

The solar power absorbed by the cooling film is given by:

$$P_{sun} = A \int_0^{\infty} d\lambda \cdot I_{AM1.5}(\lambda) \cdot \epsilon(\lambda,\theta_{sun}) \tag{7}$$

where $I_{AM1.5}$ represents the solar illumination intensity of the AM1.5 spectrum of sunlight (ASTM G173-03 2020).

The power lost due to conduction and convection from the surroundings is given by:

$$P_{cond+conv} = Ah_c(T_{amb} - T) \tag{8}$$

where h_c is the combined non-radiative heat transfer coefficient that represents the effect of heating caused by conduction and convection due to contact with air and other external surfaces.

Radiative cooling is achieved when the radiative power of the cooling film is greater than the sum of the absorbed solar power, the absorbed atmospheric thermal radiative power, and the lost power due to conduction and convection.

The emissivity of the overall film structure is required to calculate the net radiative power generated by the structure. According to Kirchhoff's law of thermal radiation, the emissivity of a material can be considered equal to its absorptivity. The absorptivity of a material or film varies with the wavelength of light or radiation incident on it, as some materials absorb more radiation at different wavelengths. The distribution of absorptivity with wavelength can be acquired by using the transfer matrix method. The transfer matrix method is based on a complex set of equations that generates the spectral variation of absorptivity vs wavelength of light for a structure by using the data of the refractive indices and extinction coefficients of the materials within the structure. A mathematical model (Aaron 2020) of the transfer matrix method can be used to generate the spectral plot of absorptivity vs wavelength for a thin-layered film.

The inputs required for the model include the refractive index and extinction coefficient data, the thickness of each layer of material within the film, as well as the angle of incidence of light on the film. The plot generated by the model shows the absorptivity, reflectance, and transmittance of the film with respect to the wavelength of light.

Based on Eqs. (1–8), there are a set of conditions that need to be satisfied for radiative cooling to be achieved. Firstly, it must reflect sunlight strongly in the visible and near-infrared spectrum, to minimize the solar power absorbed by the cooling device. Secondly, it should emit radiation greatly in the transparent wavelength ranges of the atmosphere, and it is preferred if it is able to absorb throughout the infrared region of radiation. Lastly, the film should be well sealed from the environment, which would minimize the non-radiative heat transfer coefficient to help maximize cooling power (Raman et al. 2014).

A radiative cooling film or coating consists of different materials that can be structured in different ways. The final structure is also known as a photonic film, as it can selectively manipulate light particles. A cooling film that consists of different layers of materials that vary only in one direction is known as a one-dimensional photonic film. Likewise, a variation in 2 directions is two-dimensional, and if the structure varies in all 3 directions, it is three-dimensional. The following research focuses on the use of one-dimensional film structures for radiative cooling.

2.2 Relevant research

In the beginning, pigmented paints were the first coatings or films used for radiative cooling. In 1978, Harrison and Walton were the first to achieve daytime radiative cooling of 2 °C below the ambient temperature, by using white pigmented paints of titanium dioxide (TiO_2) (Harrison and Walton 1978). The next major advancement in this field was achieved by a study published in 2013 (Rephaeli et al. 2013). In this study, a 2D metal-dielectric photonic structure was devised which was capable of daytime radiative cooling with a significant cooling performance. In 2014, Raman et al. (2014) presented a one-dimensional photonic film that consists of seven alternate layers of silicon dioxide and hafnium dioxide with certain thicknesses on top of a silver substrate, as shown in Fig. 1. It was experimentally found that this radiative cooling film was able to cool to 4.5 °C below ambient temperature, thus showing that daytime radiative cooling is possible.

Silicon dioxide is used as it has a property of high phonon-polariton resonance, which causes higher emission of infrared radiation in the 8–13 µm wavelength range of light. Hafnium dioxide also has high infrared emission in the 8–13 µm range and has low ultraviolet absorption, which helps in optimizing for solar reflectance. Additionally, SiO_2 has a low refractive index, whereas HfO_2 has a high refractive index. The combination of alternating high and low refractive indices results in interference that increases the emission of infrared radiation even further. Ag is used as it has a useful property of high solar reflectance, which decreases the absorption of solar energy. After this study, the use of one-dimensional films for radiative cooling has been an active research topic, with considerable progress since then.

The following research after this involved experimenting with other materials to further optimize radiative cooling. In 2016, Chen et al. (2016) used layers of silicon nitride, silicon, and aluminum of certain thicknesses to construct an ideally selective emitter in the atmospheric transparent window. This film structure is shown in Fig. 2. Silicon nitride is used due to its similar property of high phonon-polariton resonance, which along with silicon increases emission in the transparent window of the atmosphere. Aluminium is used for the bottom layer as a solar reflector, due to favorable reflective properties.

In 2017, a film structure was designed in a study (Kecebas et al. 2017) with 7 alternating layers of silicon dioxide and titanium dioxide with a bottom silver layer as shown in Fig. 3. Titanium dioxide is optically similar to hafnium dioxide, as it has a high refractive index with high infrared emission. As such, the film structure shown in Fig. 3 also consists of low and high index materials that utilize phonon-polariton resonance to increase infrared emission. This film structure can lower its temperature to 5 °C below ambient temperature and has a radiative cooling power of 100 W/m^2. In this study, the cooling power and temperature reduction were found using a mathematical model without any experimentation, which is the basis for the methodology of this project. The use of the mathematical model shows that the thicknesses of the emitting layers are important, and the surroundings of the film structure affect the cooling power as well.

Further research in the field involves the use of polymers. The first experimental investigation of using polymers (Long Kou et al. 2017) consists of a film structure that includes a polymer known as polydimethylsiloxane (PDMS) as the top layer, silicon as the middle layer, and a silver film as the bottom reflector (Fig. 4). The PDMS layer is optically transparent to the wavelengths of light that need to be reflected and when coupled with silica (SiO_2), it helps in increasing the infrared emission in the atmospheric window. The cooling performance of this film is found to be significantly higher than previous research and ranges from 127 to 158 W/m^2.

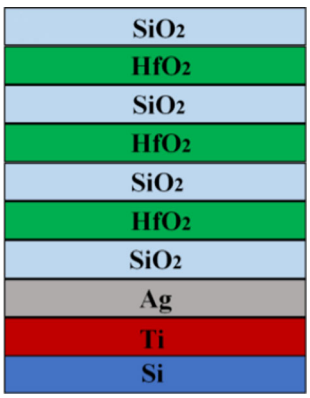

Fig. 1 HfO_2/SiO_2 multi-layer on Ti (Ko et al. 2018; Raman et al. 2014)

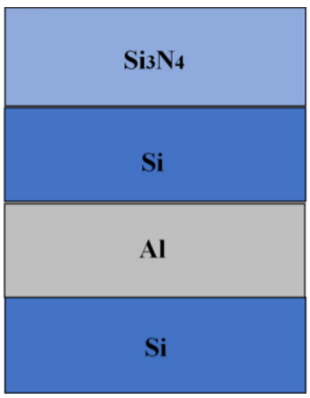

Fig. 2 Si_3N_4/Si/Al on Si (Ko et al. 2018; Chen et al. 2016)

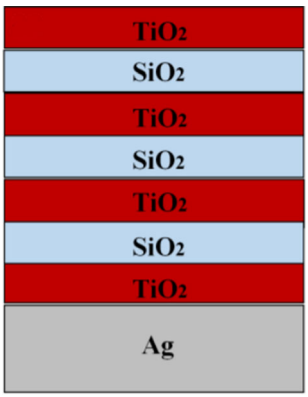

Fig. 3 SiO_2/TiO_2 multi-layer on a metallic Al/Ag reflector (Ko et al. 2018; Kecebas et al. 2017)

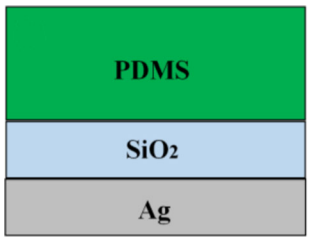

Fig. 4 PDMS/SiO_2 on Ag (Ko et al. 2018; Long Kou et al. 2017)

In another study (Yang et al. 2018), polytetrafluoroethylene (PTFE) is used with silver in the middle and silicon as the bottom layer as shown in Fig. 5. PTFE has high reflectance in the range of ultraviolet to near-infrared wavelengths, and in combination with the emitting silicon layer and reflecting silver layer, radiative cooling was achieved up to 11 °C below the ambient temperature.

In general, research has shown that a polymer layer improves the effect of the main reflective and emissive layers (Long Kou et al. 2017; Yang et al. 2018; Suichi et al. 2018; Zhai 2017). However, the studies performed on radiative cooling devices consisting solely of inorganic materials to obtain a high performance like that of polymer-based films are limited (Jeong et al. 2020a). Polymer-based radiative structures have a shorter life span due to oxidation and degeneration when exposed to sunlight for longer periods (Jeong et al. 2020b). Furthermore, polymers used as infrared emissive layers can gradually turn yellow

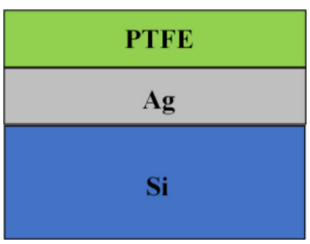

Fig. 5 PTFE/Ag on Si (Ko et al. 2018; Yang et al. 2018)

when exposed to the environment for longer periods (Jeong et al. 2020a). As such, radiative cooling systems comprised entirely of inorganic materials are beneficial in terms of the lifespan of the device.

3 Design and optimization

There are certain preferred design conditions according to which the materials for the thin-film structure are selected. For the top layers of the structure, the materials are selected such that they are highly emissive in the infrared region of the spectrum, to maximize infrared radiation and cooling power. The middle layers were chosen to be consisting of alternating layers of two materials; a high index and a low index material, which also exhibit phonon-polariton resonance in the 8–13 μm range of radiation. Alternating high and low index layers of such materials produce interference effects, which maximizes the reflection of solar radiation and emission of infrared radiation (Raman et al. 2014; Kecebas et al. 2017).

The final bottom layer was chosen to be a solar reflective layer, which would reflect wavelengths containing solar power. The materials selected also need to be transparent so that radiation can pass through them. Based on these conditions, four materials were considered for the design of the thin film: Silicon dioxide, Silicon Nitride, Aluminum Oxide, and Silver. The data of the refractive index and extinction coefficient of these materials were obtained from an experimental study (Kischkat 2012).

Silicon dioxide (SiO_2): Silicon dioxide is an optically transparent, low refractive index, inorganic material that has high absorption and emission in the atmospheric window of infrared radiation (Raman et al. 2014). The refractive index of silicon dioxide at a wavelength of 550 nm is equal to 1.46 (Malitson 1965). Figure 6 shows the absorption spectrum of SiO_2 for a thickness of 500 nm.

Figure 6 also shows an absorption peak at around a wavelength of 9.5 μm, which is within the infrared region of the radiation spectrum. The material is selected as it can be used as the low refractive index layer for the middle layers and can also be used within the top emissive layers.

Silicon Nitride (Si_3N_4): Silicon Nitride is a high refractive index inorganic material that also has high absorption in the infrared region of radiation (Liang et al. 2020). The refractive index of silicon nitride at a wavelength of 550 nm is equal to 2.0523 (Luke et al. 2015). Figure 7 shows the absorption spectrum of Si_3N_4 for a thickness of 500 nm.

From the plot, it can be observed that there is an absorption peak at a wavelength of around 11 μm, which is also present within the infrared region of radiation. The absorption also persists beyond the atmospheric

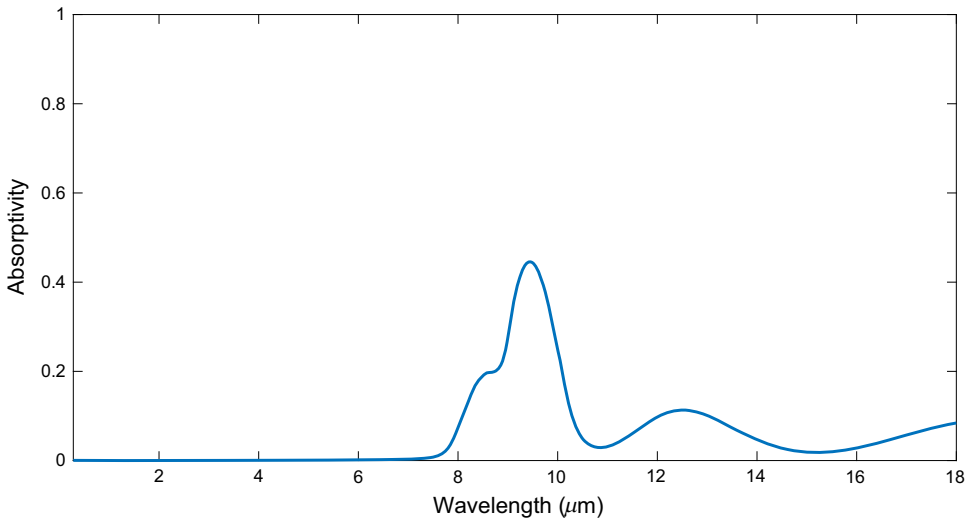

Fig. 6 Absorption spectrum of SiO_2 (silicon dioxide)

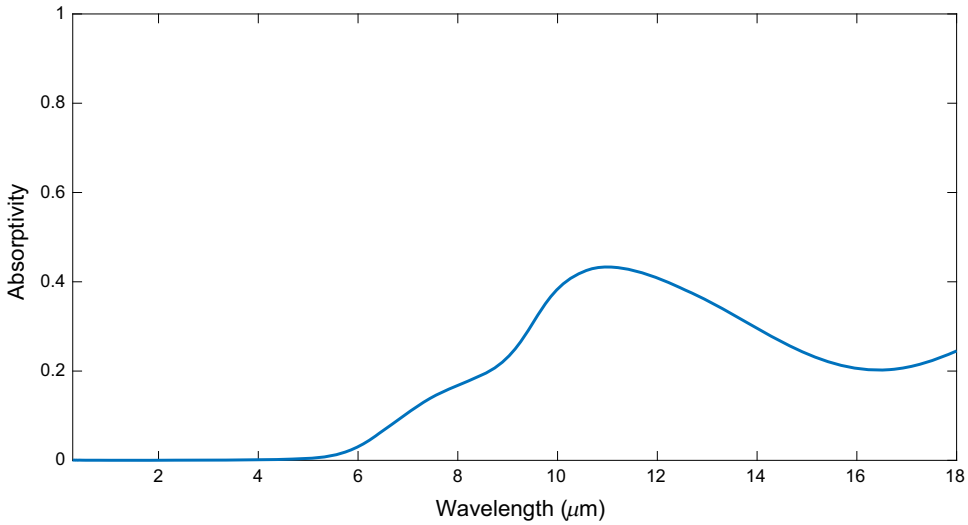

Fig. 7 Absorption spectrum of Si_3N_4 (silicon nitride)

transparency window. This material is selected as it can be used as the high refractive index layer for the middle layers of the structure and can also be used as a thicker emissive layer within the top region of the structure.

Aluminum oxide (Al_2O_3): It is a medium refractive index inorganic material that also has high absorption in the infrared region of the spectrum (Eriksson et al. 1981). The refractive index of aluminum oxide at a wavelength of 550 nm is equal to 1.6825 (Boidin et al. 2016). Figure 8 shows the absorption spectrum of Al_2O_3 for a thickness of 500 nm.

Figure 8 shows that the absorption peak is at a wavelength of around 13 μm, which is at the farther end of the atmospheric transparency window. The material helps in the absorption of higher wavelengths of radiation, which would help in increasing the cooling power of the material. It is selected to be used as a thick layer for the top region of the film structure.

Silver (Ag): Silver as a thin film possesses high reflectance throughout the spectrum of electromagnetic radiation (Kecebas et al. 2017). Figure 9 shows the reflectance of silver for a thickness of 200 nm.

This material is considered for the bottom layer as a reflector of solar radiative power. By increasing the reflectance, it helps to keep the absorption low in the wavelength range of 280–4000 nm, as the other selected materials have no absorption within this wavelength range of the spectrum.

The final design approach is to use Silver as the bottom layer for solar reflection; Silicon dioxide and Silicon nitride as the alternating low and high refractive index materials for the thinner middle layers; and silicon dioxide, silicon nitride, and aluminum oxide as materials for the upper thick layers. Additionally, silicon is selected to be the material for the substrate of the thin film. The materials selected are inorganic and are easily available. Combining

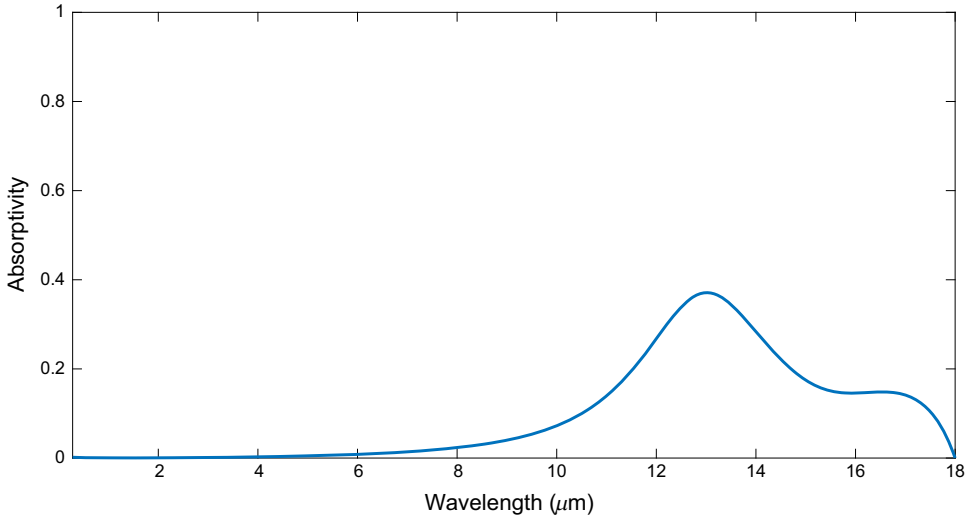

Fig. 8 Absorption spectrum of Al_2O_3 (aluminium oxide)

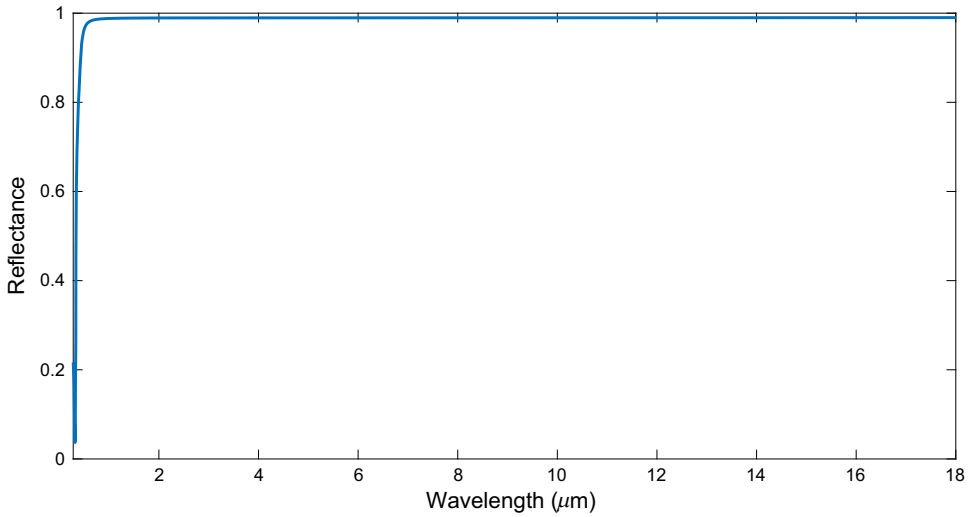

Fig. 9 Reflectance spectrum of Ag (silver)

the layers helps in maximizing the infrared emission of the structure. These inorganic materials also provide a longer lifespan to the cooler, as they are chemically stable and inert materials that do not react with the surroundings (Nalwa 2001). Also, the film structure is easier to fabricate as it is one-dimensional, as compared to other previous studies that involve complex two or three- dimensional layers within the film structures (Rephaeli et al. 2013; Zhai 2017; Gentle and Smith 2010; Huang and Ruan 2017; Bao et al. 2017; Wu 2018; Atiganyanun 2018; Mandal 2018; Hervé et al. 2018).

After the selection of the materials, the arrangement of the materials and the thicknesses of the layers are improved using an optimization method. The method used is known as the needle optimization method (Tikhonravov et al. 1996). It aims to improve the spectral distribution of a material structure, to maximize the cooling power produced by the thin film structure. The optimization procedure is performed using an open-source software (Larouche and Martinu 2008).

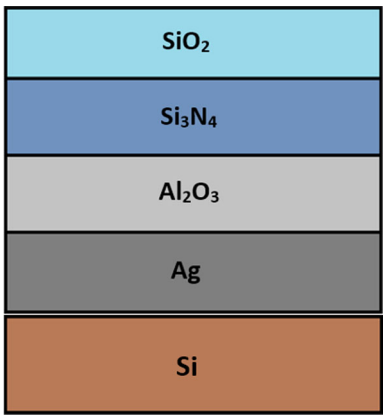

Fig. 10 Initial design of the material structure

The initial design of the material structure is shown in Figs. 10, and 14 shows the spectrum for the initial arrangement of the layers. The thicknesses of all the layers are initially set as 200 nm. To improve the spectral distribution of absorption, the optimization is performed in steps as shown in Fig. 11. The first step for the starting design is to identify the points in the initial arrangement to insert new layers. In the first step, one needle is added to the spectrum in the system, which identifies the points in the structure to insert new layers. The second step improves the spectrum by adding 2 layers of any of the initially selected materials, and by optimizing the thicknesses of all the layers.

The steps are repeated by inserting new layers until there is no further improvement in the absorption spectrum of the material structure. At this point, the final design and absorption spectrum of the thin film is attained. The needle optimization method can be represented by a flowchart as shown in Fig. 11.

4 Validation of methodology

The methodology used for the calculations is validated by using it to calculate the relevant values of a research paper (Kecebas et al. 2017). Table 1 shows the values of the relevant parameters and the error between the calculated and research values.

Figure 12 shows the spectral plot of absorption versus wavelength from the research paper, and Fig. 13 shows the plot of absorptivity versus wavelength acquired by using the mathematical model for the same configuration of the material structure specified in the research paper (Table 2).

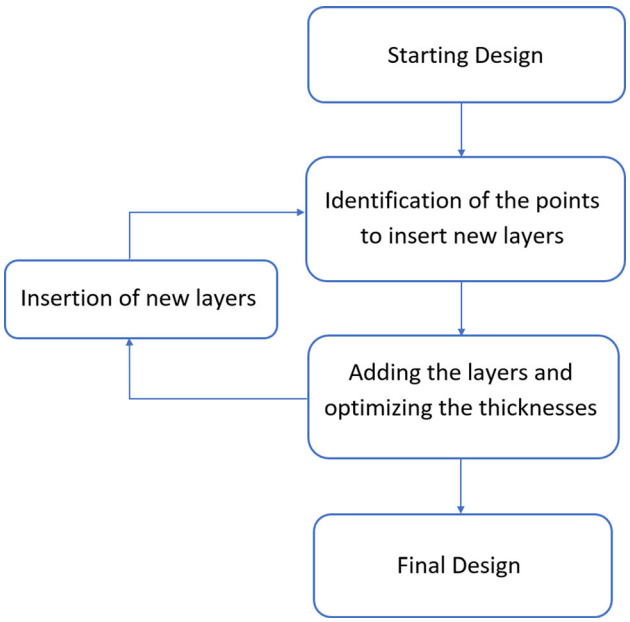

Fig. 11 General flowchart of the design procedure based on the needle optimization method (Tikhonravov et al. 1996)

It can be observed that the absorption spectrums above are notably similar in terms of the distribution of the absorption over the wavelength, which confirms the methodology used to obtain the relevant spectral plots. Furthermore, the optimization of the initial design is performed using an open-source validated software (Larouche and Martinu 2008), which ensures that the results of the optimization are accurate. Therefore, based on high similarity of the calculated results with the results of a previously performed study, the methodology used for the design and calculations of the project has been validated.

5 Results and discussion

5.1 Final design

The results of the design and optimization are displayed in Figs. 14, 15, 16, 17, 18 and 19, which show the absorption spectrums at different stages of optimization, each having a different number of layers. Improvements can be observed in the spectral distribution after each stage of optimization. The emission in the infrared range increases for each successive stage while the emissivity in the solar spectrum range (280–4000 nm) remains minimum.

As the number of layers of the selected materials within the design increase, the spectrum is further improved. The largest increase in emission/absorption can be noted after the first optimization when the thicknesses of the initial design are optimized. The emissivity and reflectance then gradually increase with the number of layers until the maximum values are reached, after which further optimization does not contribute any significant improvement.

Figure 19 shows the absorption spectrum of the final design of the thin film structure. The final design of the thin film consists of 10 layers of varying thicknesses. The absorption spectrum has insignificant improvement if further layers are inserted into the design of the thin film at this stage.

From the plot in Fig. 19, an average emissivity of 0.945 exists in the atmospheric window of infrared radiation between 8 and 13 μm. Also, an average reflectance of 0.963 exists in the solar radiation spectrum. As a result, the structure can emit a significant portion of infrared radiation while reflecting most of the solar radiation incident upon it.

The transmissivity throughout the entire spectrum is equal to zero, which helps to focus on the improvement of the absorption and reflection of the structure. Figure 20 shows the final design of the thin film structure. The thicknesses of the layers from top to bottom are 125 nm, 210 nm, 1624 nm, 614 nm, 1063 nm, 52 nm, 29 nm,

Table 1 Comparison of research and calculated values for validation

Parameter	Research value (Santamouris and Feng 2018)	Calculated value	Percentage error (%)
Emissivity/absorptivity (8–13 μm)	0.45	0.44	2.22
Emissivity/absorptivity (280–4000 nm)	0.03	0.028	6.66
Reflectance (280–4000 nm)	0.97	0.972	0.20
Net cooling power density (W/m^2)	35	38	8.5

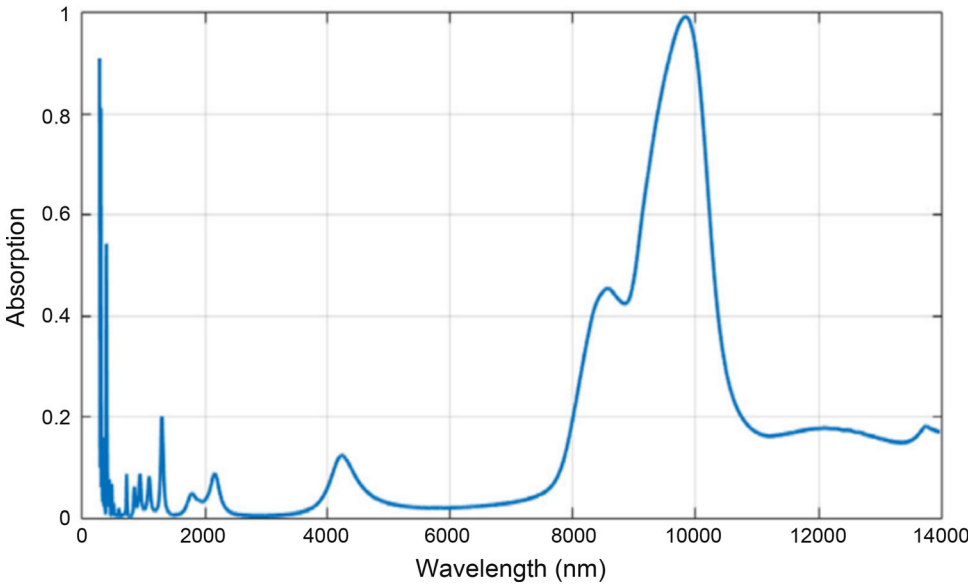

Fig. 12 Absorption spectrum of the research paper (Kecebas et al. 2017)

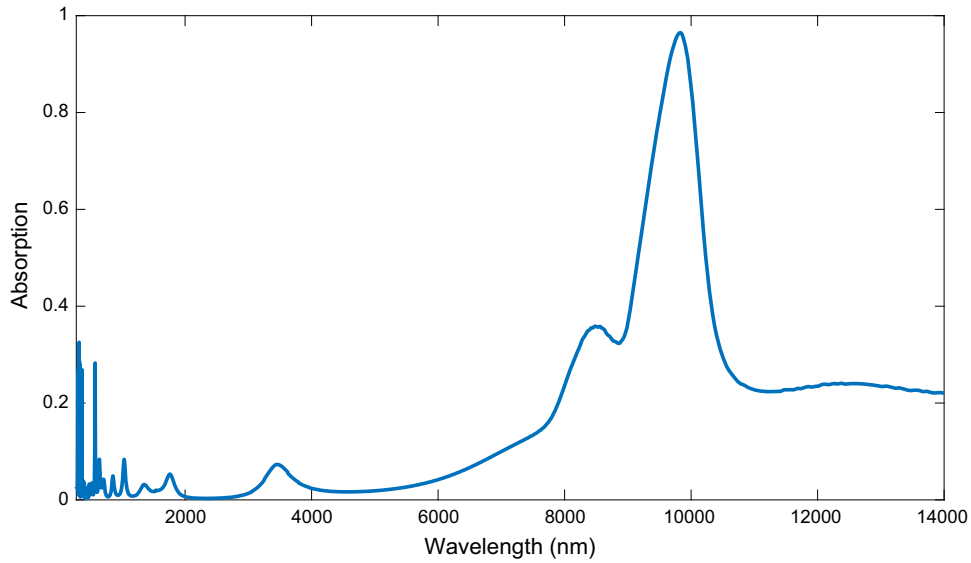

Fig. 13 Absorption spectrum obtained using methodology

60 nm, 48 nm, and 200 nm, respectively. The total thickness of the final optimized thin film is equal to 4025 nm. From the results of the optimization, it can be noted that the emissivity and reflectance of the structure are highly dependent on the thicknesses of the layers, and a slight change in the thicknesses can greatly affect the values of emissivity and reflectance.

In general, the final design of the one-dimensional inorganic photonic thin film consists of five upper, relatively thicker layers that are highly emissive in the infrared

Table 2 Emissivity and reflectance for the stages of optimization

Stage of optimization	No. of layers	Reflectance (280–4000 nm)	Emission/absorption in 8–13 μm range of wavelength
0	4	0.966	0.2047
1	4 (thicknesses optimized)	0.955	0.7768
2	6	0.958	0.8367
3	8	0.961	0.8936
4	9	0.963	0.9051
5	10 (final design)	0.963	0.9457

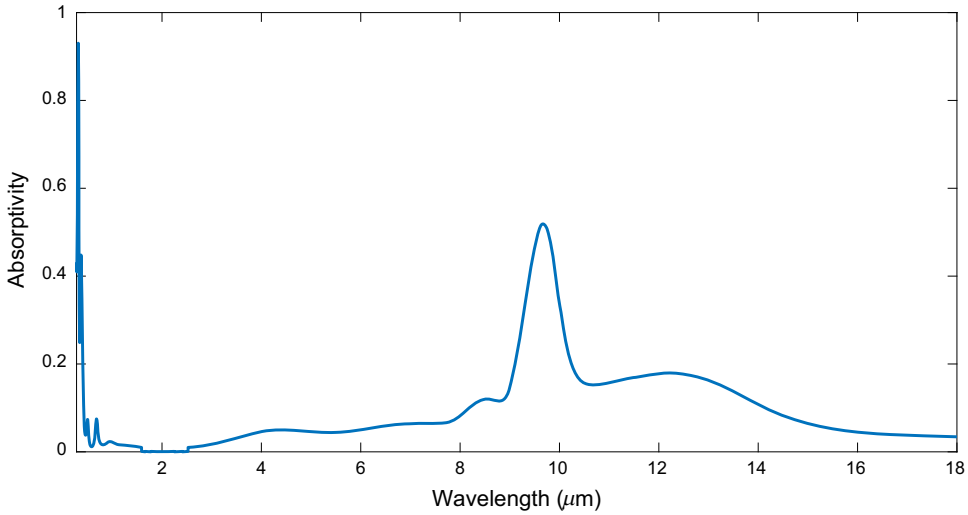

Fig. 14 No. of layers: 4 (initial design)

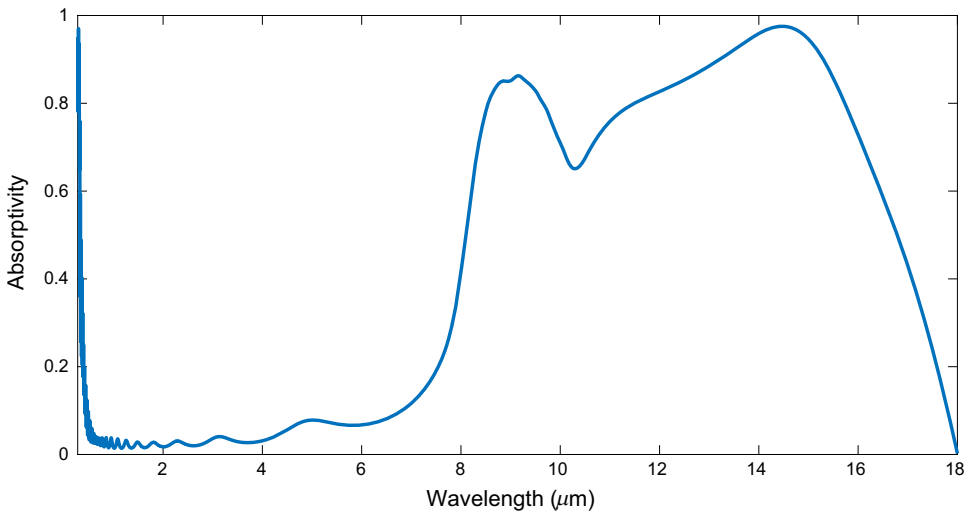

Fig. 15 No. of layers: 4 (thicknesses optimized)

range of the spectrum. The upper layers are followed by four relatively thinner layers of alternating low (SiO_2) and high (Si_3N_4) refractive index layers which contribute to high absorption in the infrared region. The bottom layer consists of a highly reflective material (Ag) that provides high reflectance in the solar spectrum of radiation.

5.2 Cooling Performance Analysis

The equations from the methodology are incorporated into the mathematical model to calculate the amount of cooling power the thin film can produce. The cooling power of the thin film is calculated using the model and is found to be

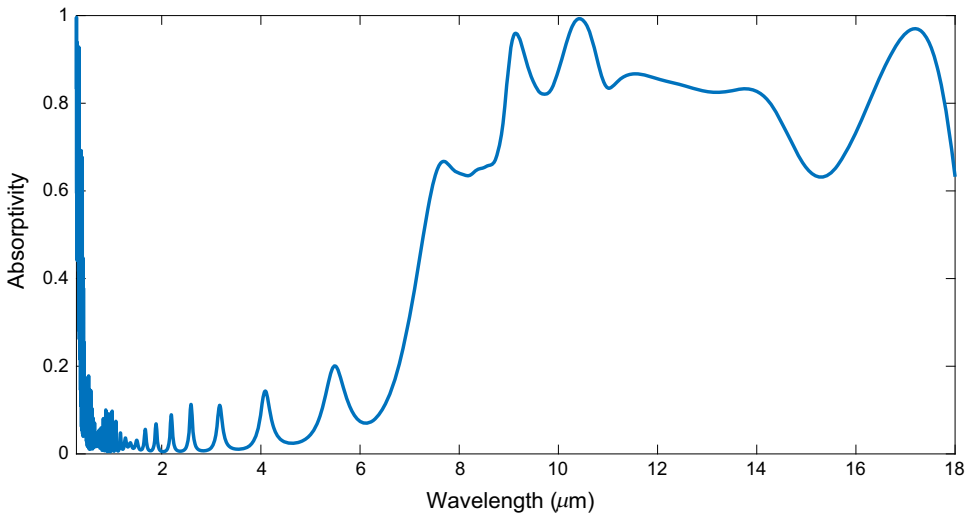

Fig. 16 No. of layers: 6

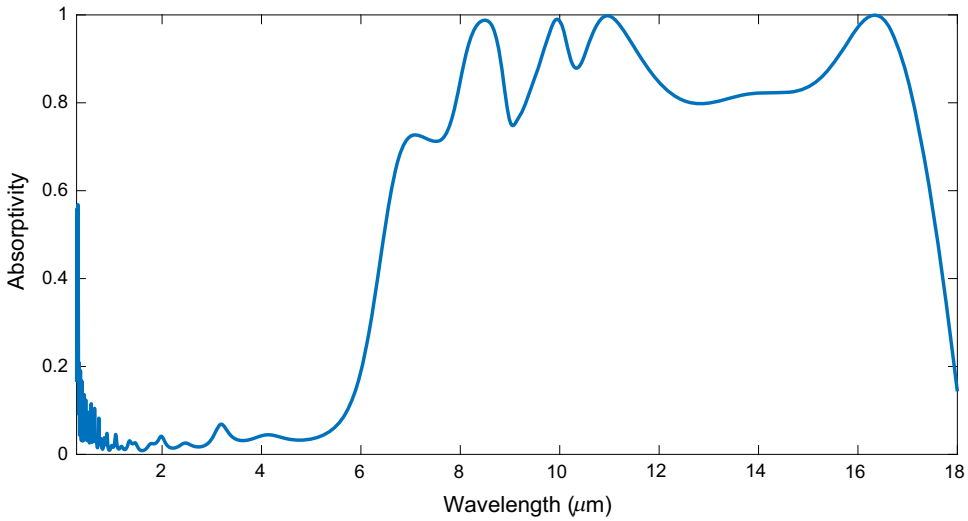

Fig. 17 No. of layers: 8

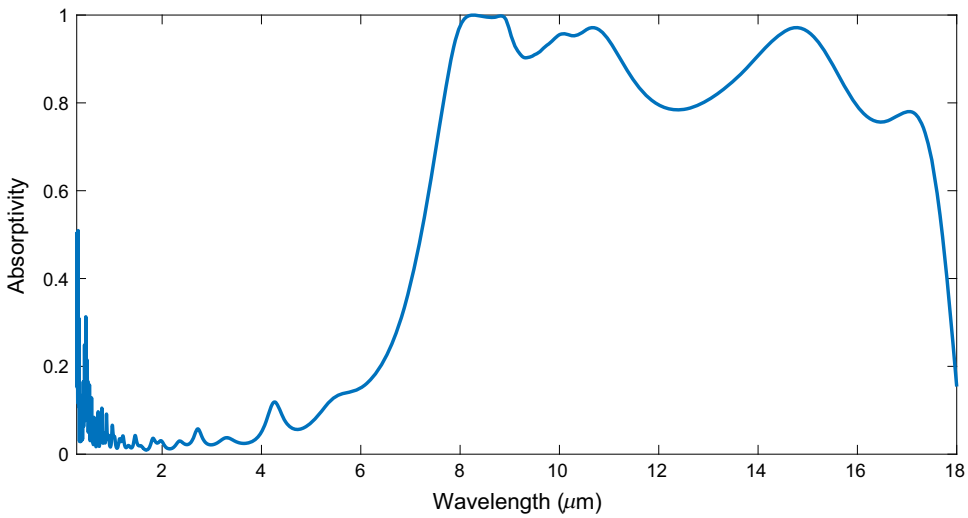

Fig. 18 No. of layers: 9

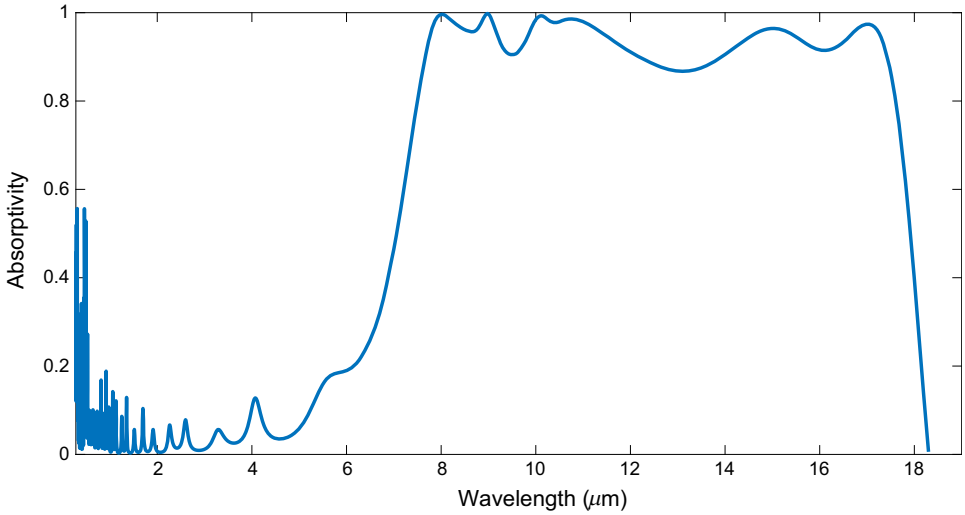

Fig. 19 No. of layers: 10 (final design)

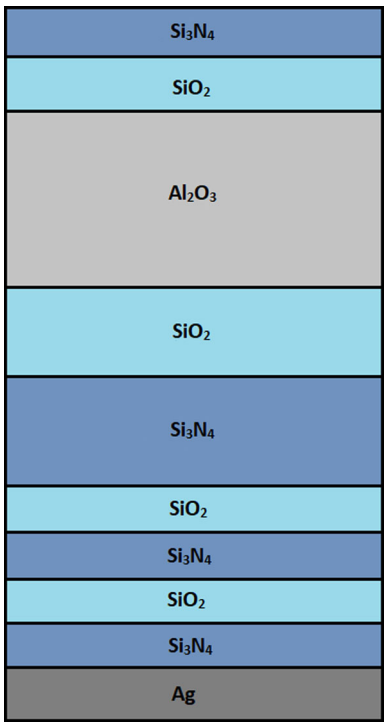

Fig. 20 Final design of the thin film material structure

equal to 125 W/m^2 during daytime when both the surface temperature of the film and the ambient temperature are equal to 300 K. High broadband emission is achieved in the atmospheric transparency window using the optimized film material structure. The emissivity of the structure in the atmospheric transparency window is equal to 0.945, which means it emits 94.5% of the absorbed radiation within that region. Overall, the proposed multilayered structure generally has a better performance than that of previously proposed structures (Jeong et al. 2020a).

The average emissivity of the structure within the transparency window for different angles of incidence of radiation on the structure is represented by Fig. 21. The emissivity is maximum for an angle of zero degrees on the film and decreases gradually as the angle of incidence with respect to the normal approaches 90°. This occurs because the emissivity of a structure is dependent on the angle of incidence, and the portion of radiation emitted by a surface is lesser at a wider angle.

Figure 22 shows the variation of the net cooling power density generated as a function of the surface temperature of the material structure. An ambient temperature of 300 K was used for the plot shown in Fig. 22. As the temperature of the surface decreases, the cooling performance decreases until it reaches zero and thermal equilibrium is attained. The effect of non-radiative heat transfer on the cooling performance is also investigated. Three varying values of non-radiative heat transfer coefficient which include h_c = 0, 6, 12 W/m^2 K are considered. The line of $h_c = 0$ shows the cooling performance when heat loss due to convection and conduction with the surroundings is zero, and h_c = 6, 12 represent convective heat loss when the airspeed with respect to the surface is approximately equal to 1 m/s and 3 m/s respectively (Huang and Ruan 2017).

The equilibrium temperatures for combined conductive and convective heat transfer coefficients of 0, 6, 12 W/m^2 K are approximately equal to 260, 286, and 291 K respectively. The cooling power of the designed film structure was calculated to be equal to 125 W/m^2 under direct solar radiation at an ambient temperature of 300 K. Another observation is that the cooling power is not affected by the non-radiative heat transfer if the temperature of the surface is equal to the ambient temperature, as the heat loss due to convection and conduction will be zero for this case.

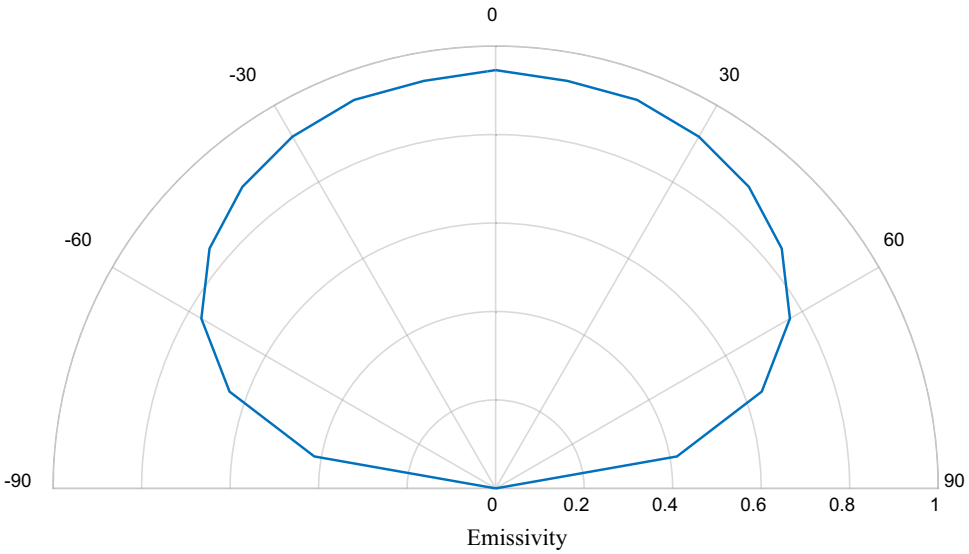

Fig. 21 Polar plot showing the dependence of emissivity of the structure on the angle of incidence

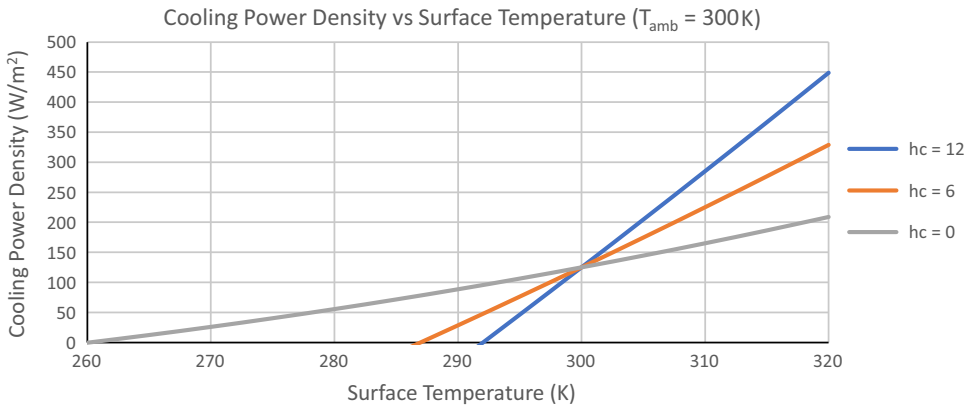

Fig. 22 Variation of cooling power density with the surface temperature of the material structure

When the surface temperature is higher than the ambient temperature, the cooling performance will be even higher for a greater convective coefficient as convection will increase the cooling effect. However, when the ambient temperature is higher than the surface temperature, the convective effect results in heating of the surface, and the cooling performance as such will be lesser. To conclude, the final result achieved is that for a practical non-radiative heat transfer coefficient of 12 W/m^{2}K, the temperature reduction from ambient during daytime is approximately equal to 8 °C, and the cooling performance achieved at ambient temperature is equal to 125 W/m^2.

Several prohibiting factors also exist in the field of passive daytime radiative cooling, such as high material and fabrication costs, the effect of varying weather conditions on the cooling performance, and instability when exposed to sunlight for long periods (Jeong et al. 2020a).

6 Conclusion

In this work, a multilayered inorganic structure is proposed for passive daytime radiative cooling. The four materials considered for the structure were silicon dioxide, silicon nitride, aluminium oxide, and silver on top of a silicon substrate, and a specific arrangement of these layers was designed and optimized to achieve a high-performance daytime radiative cooling material structure. As the materials are inorganic, the final structure is mechanically and chemically stable in exterior environments even after being exposed to sunlight for long periods, as opposed to organic structures that exhibit a decrease in performance when exposed to sunlight for longer periods. The final structure is also one-dimensional, due to which it can be fabricated relatively easily as compared to two or three-dimensional

structures. Furthermore, the final structure can be fabricated on a substrate using various techniques such as ion beam deposition, vacuum deposition, and electron beam evaporation (Raman et al. 2014; Kecebas et al. 2017; Long Kou et al. 2017).

The proposed structure has high emission within the infrared region of the spectrum and can emit radiation that is able to pass through the atmosphere and into cold outer space. Moreover, the proposed structure can be potentially used for applications such as space cooling of building HVAC systems, passive cooling of solar cells (Babu et al. 2020), and radiation of heat energy absorbed from appliances when in direct contact through conduction. A net cooling performance of 125 W/m^2 can be achieved by the structure based on calculations, which is relatively high compared to previous studies (Jeong et al. 2020a).

For future work, the proposed structure can be fabricated and experimentally tested to measure the cooling performance of the structure in realistic conditions. After fabrication and testing, it can be used as a mechanism to absorb heat energy through conduction from a heat source such as an evaporator and radiate the absorbed heat through the atmosphere and into outer space.

References

Aaron H (2020) Rose, "RTACalc—File Exchange—MATLAB Central. https://www.mathworks.com/matlabcentral/fileexchange/69355-rtacalc. Accessed 15 Aug 2020.

ASTM G173-03 (2020) Standard tables for reference solar spectral irradiances: direct normal and hemispherical on 37° tilted surface. https://www.astm.org/Standards/G173.htm. Accessed 26 Aug 2020

Atiganyanun S et al (2018) Effective radiative cooling by paint-format microsphere-based photonic random media. ACS Photonics 5(4):1181–1187. https://doi.org/10.1021/acsphotonics.7b01492

Babu E, Yesudasan S, Chacko S (2020) Cymatics inspired self-cleaning mechanism for solar panels. Microsyst Technol. https://doi.org/10.1007/s00542-020-04978-4

Bao H, Yan C, Wang B, Fang X, Zhao CY, Ruan X (2017) Double-layer nanoparticle-based coatings for efficient terrestrial radiative cooling. Sol Energy Mater Sol Cells 168:78–84. https://doi.org/10.1016/j.solmat.2017.04.020

Berdahl P, Martin M, Sakkal F (1983) Performances thermiques des panneaux a refroidissement radiatif. Int J Heat Mass Transf 26(6):871–880. https://doi.org/10.1016/S0017-9310(83)80111-2

Boidin R, Halenkovič T, Nazabal V, Beneš L, Němec P (2016) Pulsed laser deposited alumina thin films. Ceram Int 42(1):1177–1182. https://doi.org/10.1016/j.ceramint.2015.09.048

Chen Z, Zhu L, Raman A, Fan S (2016) Radiative cooling to deep sub-freezing temperatures through a 24-h day-night cycle. Nat Commun 7(1):1–5. https://doi.org/10.1038/ncomms13729

Daisy SY (2016) Molecular dynamics study of solid-liquid heat transfer and passive liquid flow. Ph.D. Thesis Syracuse University, Syracuse, USA

Eriksson TS, Hjortsberg A, Niklasson GA, Granqvist CG (1981) Infrared optical properties of evaporated alumina films. Appl Opt 20(15):2742. https://doi.org/10.1364/ao.20.002742

Gentle AR, Smith GB (2010) Radiative heat pumping from the Earth using surface phonon resonant nanoparticles. Nano Lett 10(2):373–379. https://doi.org/10.1021/nl903271d

Goldstein EA, Raman AP, Fan S (2017) Sub-ambient non-evaporative fluid cooling with the sky. Nat Energy 2(9):1–7. https://doi.org/10.1038/nenergy.2017.143

Harrison AW, Walton MR (1978) Radiative cooling of TiO_2 white paint. Sol Energy 20(2):185–188. https://doi.org/10.1016/0038-092X(78)90195-0

Hervé A, Drévillon J, Ezzahri Y, Joulain K (2018) Radiative cooling by tailoring surfaces with microstructures: association of a grating and a multi-layer structure. J Quant Spectrosc Radiat Transf 221:155–163. https://doi.org/10.1016/j.jqsrt.2018.09.015

Hossain MM, Gu M (2016) Radiative cooling: principles, progress, and potentials. Adv Sci. https://doi.org/10.1002/advs.201500360

Hotchandani V, Mathew B, Yesudasan S, Chacko S (2020) Thermo-hydraulic characteristics of novel MEMS heat sink. Microsyst Technol. https://doi.org/10.1007/s00542-020-04933-3

Huang Z, Ruan X (2017) Nanoparticle embedded double-layer coating for daytime radiative cooling. Int J Heat Mass Transf 104:890–896. https://doi.org/10.1016/j.ijheatmasstransfer.2016.08.009

Jeong SY, Tso CY, Zouagui M, Wong YM, Chao CYH (2018) A numerical study of daytime passive radiative coolers for space cooling in buildings. Build Simul 11(5):1011–1028. https://doi.org/10.1007/s12273-018-0474-4

Jeong SY et al (2020a) Field investigation of a photonic multi-layered TiO_2 passive radiative cooler in sub-tropical climate. Renew Energy 146:44–55. https://doi.org/10.1016/j.renene.2019.06.119

Jeong SY, Tso CY, Wong YM, Chao CYH, Huang B (2020b) Daytime passive radiative cooling by ultra emissive bio-inspired polymeric surface. Sol Energy Mater Sol Cells 206:110296. https://doi.org/10.1016/j.solmat.2019.110296

Kecebas MA, Menguc MP, Kosar A, Sendur K (2017) Passive radiative cooling design with broadband optical thin-film filters. J Quant Spectrosc Radiat Transf 198:1339–1351. https://doi.org/10.1016/j.jqsrt.2017.03.046

Kischkat J et al (2012) Mid-infrared optical properties of thin films of aluminum oxide, titanium dioxide, silicon dioxide, aluminum nitride, and silicon nitride. Appl Opt 51(28):6789–6798. https://doi.org/10.1364/AO.51.006789

Ko B, Lee D, Badloe T, Rho J (2018) Metamaterial-based radiative cooling: towards energy-free all-day cooling. Energies 12(1):89. https://doi.org/10.3390/en12010089

Larouche S, Martinu L (2008) OpenFilters: open-source software for the design, optimization, and synthesis of optical filters. Appl Opt 47:C219–C230. https://doi.org/10.1364/AO.47.00C219

Liang Z, Shen H, Li J, Xu N (2020) Microstructure and optical properties of silicon nitride thin films as radiative cooling materials. Sol Energy 72(6):505–510. https://doi.org/10.1016/S0038-092X(02)00032-4

Long Kou J, Jurado Z, Chen Z, Fan S, Minnich AJ (2017) Daytime radiative cooling using near-black infrared emitters. ACS Photonics 4(3):626–630. https://doi.org/10.1021/acsphotonics.6b00991

Luke K, Okawachi Y, Lamont MRE, Gaeta AL, Lipson M (2015) Broadband mid-infrared frequency comb generation in a Si3N4 microresonator. Opt Lett 40:4823–4826

Malitson IH (1965) Interspecimen comparison of the refractive index of fused silica. J Opt Soc Am 55(10):1205. https://doi.org/10.1364/josa.55.001205

Mandal J et al (2018) Hierarchically porous polymer coatings for highly efficient passive daytime radiative cooling. Science 362(6412):315–319. https://doi.org/10.1126/science.aat9513

Martin M, Berdahl P (1984) Characteristics of infrared sky radiation in the United States. Sol Energy 33(3):321–336. https://doi.org/10.1016/0038-092X(84)90162-2

Nalwa HS (2001) Silicon-based material and devices: materials and processing, properties and devices. Elsevier Science, Burlington

Noronha B, Yesudasan S, Chacko S (2020) Static and dynamic analysis of automotive leaf spring: a comparative study of various materials using ANSYS. J Fail Anal Preven 20:804–818. https://doi.org/10.1007/s11668-020-00877-y

Raman AP, Anoma MA, Zhu L, Rephaeli E, Fan S (2014) Passive radiative cooling below ambient air temperature under direct sunlight. Nature 515(7528):540–544. https://doi.org/10.1038/nature13883

Rephaeli E, Raman A, Fan S (2013) Ultrabroadband photonic structures to achieve high-performance daytime radiative cooling. Nano Lett 13(4):1457–1461. https://doi.org/10.1021/nl4004283

Santamouris M, Feng J (2018) Recent progress in daytime radiative cooling: is it the air conditioner of the future? Buildings 8(12):168. https://doi.org/10.3390/buildings8120168

Suichi T, Ishikawa A, Hayashi Y, Tsuruta K (2018) Performance limit of daytime radiative cooling in warm humid environment. AIP Adv 8(5):055124. https://doi.org/10.1063/1.5030156

Sumith YD, Maroo SC (2015) Surface-heating algorithm for water at nanoscale. J Phys Chem Lett 6(18):3765–3769. https://doi.org/10.1021/acs.jpclett.5b01627

Sumith YD, Maroo SC (2016) Origin of surface-driven passive liquid flows. Langmuir 32(34):8593–8597. https://doi.org/10.1021/acs.langmuir.6b02117

The Sites|Gemini Observatory (2020) https://www.gemini.edu/observing/telescopes-and-sites/sites#Transmission. Accessed 15 Aug 2020

Tikhonravov AV, Trubetskov MK, DeBell GW (1996) Application of the needle optimization technique to the design of optical coatings. Appl Opt 35(28):5493. https://doi.org/10.1364/ao.35.005493

Wang W, Fernandez N, Katipamula S, Alvine K (2018) Performance assessment of a photonic radiative cooling system for office buildings. Renew Energy 118:265–277. https://doi.org/10.1016/j.renene.2017.10.062

Wu D et al (2018) The design of ultra-broadband selective near-perfect absorber based on photonic structures to achieve near-ideal daytime radiative cooling. Mater Des 139:104–111. https://doi.org/10.1016/j.matdes.2017.10.077

Yang P, Chen C, Zhang ZM (2018) A dual-layer structure with record-high solar reflectance for daytime radiative cooling. Sol Energy 169:316–324. https://doi.org/10.1016/j.solener.2018.04.031

Yesudasan S, Chacko S (2018) Fast local pressure estimation for two dimensional systems from molecular dynamics simulations. In: Proceedings of the ASME 2018 power conference collocated with the ASME 2018 12th international conference on energy sustainability and the ASME 2018 nuclear forum. vol 2: heat exchanger technologies; plant performance; thermal hydraulics and computational fluid dynamics; water management for power systems; student competition. Lake Buena Vista, Florida, USA. June 24–28, 2018. V002T10A004. ASME. https://doi.org/10.1115/POWER2018-7263

Yesudasan S, Averett R, Chacko S (2020) Machine learned coarse grain water models for evaporation studies. Preprints, 2020070126. vol 1. https://doi.org/10.20944/preprints202007.0126

Zhai Y et al (2017) Scalable-manufactured randomized glass-polymer hybrid metamaterial for daytime radiative cooling. Science 355(6329):1062–1066. https://doi.org/10.1126/science.aai7899